Synthesis of Liquid Crystalline Polymers from Polyethylene Terephthalate and 4-Acetoxybenzoic Acid: A Kinetic Study

Ahmed Bishara, Adam Al-Mulla, Yousef Al-Roomi, Habib Shaban

Department of Chemical Engineering, Kuwait University, Safat 13060, Kuwait

ABSTRACT: Liquid crystalline polymers (LCPs) have been synthesized from polyethylene terephthalate (PET) and 4-acetoxybenzoic acid (OB) through melt step-growth polymerization. The presence of liquid crystalline texture is first examined using optical polarizing microscopy. The thermal durability of the developed systems is studied through thermogravimetric analysis. The kinetics of the polymerization processes is analyzed. The effectiveness of three catalysts commonly used in polyesterification is investigated. The effect of reaction temperature is also examined. The progress of polycondensation reactions over time takes a nonlinear behavior of slight sigmoidal shape, irrespective of whether or not the reaction is catalyzed. Simple second and third order equations, along with a nonlinear model, are used to determine the kinetic parameters characterizing these reactions. The rate of reaction is enhanced when the reaction temperature is increased. Overall, second-order kinetics well describes the polymerization reactions when the data set is divided into two regions. Antimony trioxide induces a more visible enhancement to the rate of reaction, compared to zinc acetate and sodium acetate. The presence of a catalyst generally increases the reaction activation energy. This indicates that entropy factors outweigh the increase in activation energy and drive the catalyzed reactions to completion. © 2011 Wiley Periodicals, Inc. J Appl Polym Sci 123: 1359–1369, 2012

Key words: kinetics (polym.); liquid-crystalline polymers (LCP); synthesis; activation energy; degradation

INTRODUCTION

Main-chain liquid crystal polymers (LCP) form a class of engineering materials that are used in electronic devices and fiber composites because they offer unique rheological behavior and outstanding mechanical properties. Currently, most modern, high-precision, thin-walled electronic connectors, and couplings are made from LCPs, whereas most military helmets and bulletproof vests are made from LCP fibers. In general, a polymer that exhibits liquid crystal behavior is synthesized from stiff rod-like molecules so that the long range molecular orientational order persists in the absence of various types of short range translational order. This class of ordering is a direct result of specific types of intermolecular interactions and manifests itself by unique macroscopic physical properties. The first polymer to be injection molded and characterized as actually being liquid crystalline was copolyester of polyethylene terephthalate (PET) and *p*-hydroxybenzoic acid (PHB). With the exception of the PET/PHB copolyesters, the history of synthesis of liquid crystalline polymers prior to the mid 1970s was to be limited to all-aromatic LCPs, since they had the highest overall properties of the LCPs (including superior strength and stiffness in plastics and fibers, superior thermal and oxidative stability, and greater resistance to burning than LCPs containing aliphatic spacer units).[1]

The research that led to the PET/PHB LCPs was initiated because of a desire to increase the mechanical properties, heat resistance, and fire resistance of PET fibers and plastics by increasing the aromatic content of the polymer.[1] Before the publication by F. L. Hamb of the Eastman Kodak Research Laboratories,[2] work was being carried out on the modification of PET by reaction with 4,4′- isopropylidenediphenol diacetate and an equimolar amount of terephthalic acid.

The kinetic study for polycondensation is essential for the precise quality control of the final products and process reproducibility. The kinetics is usually investigated by titrimetry of evolved acetic acid trapped in sodium hydroxide solution or monitoring the volume of acetic acid.[3–6] A number of researchers have investigated polyesterification reactions between aliphatic dibasic acids and glycols. Among them are Flory,[7] Colonge and Stuchlik,[8] Davies,[9] and Tang and Yao.[10] Flory observed that polyesterification, in the absence of a foreign acid, is a third-order reaction. Other authors,[10,11] however, pointed out

that a second-order rate equation best fit polyesterification reactions. The reaction may become third order in the later stages.

In the study of kinetics and mechanisms of polyesterifications carried out by Flory,[7] it was concluded that self-catalyzed polyesterifications follow the equation:

$$-d\,[COOH^-]/dt = k\,[COOH^-]^2\,[OH^-] \quad (1)$$

where k is the temperature-dependent rate constant. Acid-catalyzed polyesterifications follow second-order kinetics, as demonstrated by Goldschmidt[12]:

$$-d\,[COOH^-]/dt = k'\,[COOH^-]\,[OH^-] \quad (2)$$

where the rate constant k' includes the catalyst concentration. The difference in rate orders assigned to polyesterification reactions have been attributed to the influence of medium polarity.[13–18] Most studies in this area indicate that polycondensation obeys second-order kinetic, irrespective of whether the reaction is catalyzed or uncatalyzed. Under certain conditions, two kinetic regions with different reaction rate constants were observed.[3,5,6]
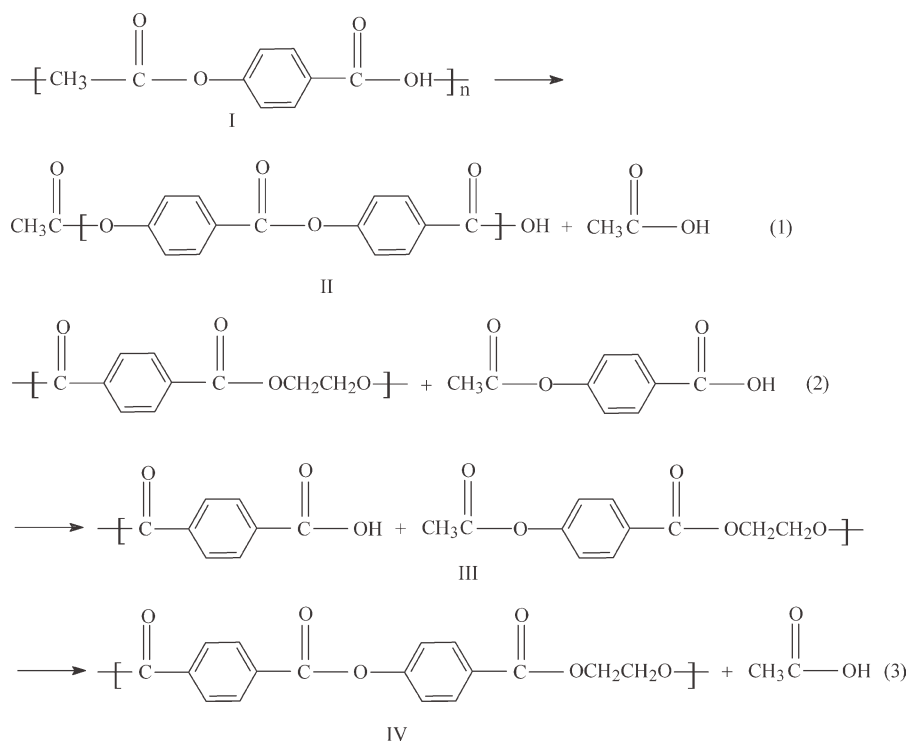
For the polycondensation of wholly aromatic polyesters, several effective catalysts are known having the capabilities of accelerating reaction as well as result in high inherent viscosity. Representative examples of catalysts suitable for these reactions are derivatives of alkali metals and alkali-earth metals such as acetates, carboxylates, and oxides of said metals. Most specifically, they can be sodium ace-

tate, sodium hydroxide, calcium benzoate, zinc oxide, antimony oxide, lead oxide, etc. Generally, the typical range of the catalytic amount is from 0.001 to 1.0 wt % based on the total monomer reactant weight.[19–24] Catalysts can affect the color and the thermal stability of the final products. But their exact role is still unknown.

Despite the fact that the synthesis of many thermoplastic polyesters has been studied since 1958,[25,26] literature on the kinetics of melt polyesterification remains somewhat scant. This is probably explained by the complexity of such reactions, originating from the high temperature needed to maintain the polymers in the molten state. Side reactions may occur at these high temperatures leading to chain growth, chain scission, changes in the chemical nature of end groups, insolubility of diacids or stoichiometric imbalances due to sublimation of reactants and diffusion constraints, all of which limit the effective removal of the side product and influence the reaction rate.

In this study, we intend to synthesize liquid crystalline polymers based on polyethylene terephthalate (PET) and 4-acetoxybenzoic acid (OB) and perform a kinetic study on the polymerization process. To the best of our knowledge, the use of second-order rate equations with breaks and the nonlinear model has not been used in the characterization of LCPs synthesized from poly (ethylene terephthalate) and 4-acetoxybenzoic acid. The findings of this study will add to the accumulated knowledge in the field of synthesis and improvement of liquid crystalline polymers.

The proposed mechanism for the reaction between PET and OB is described below:
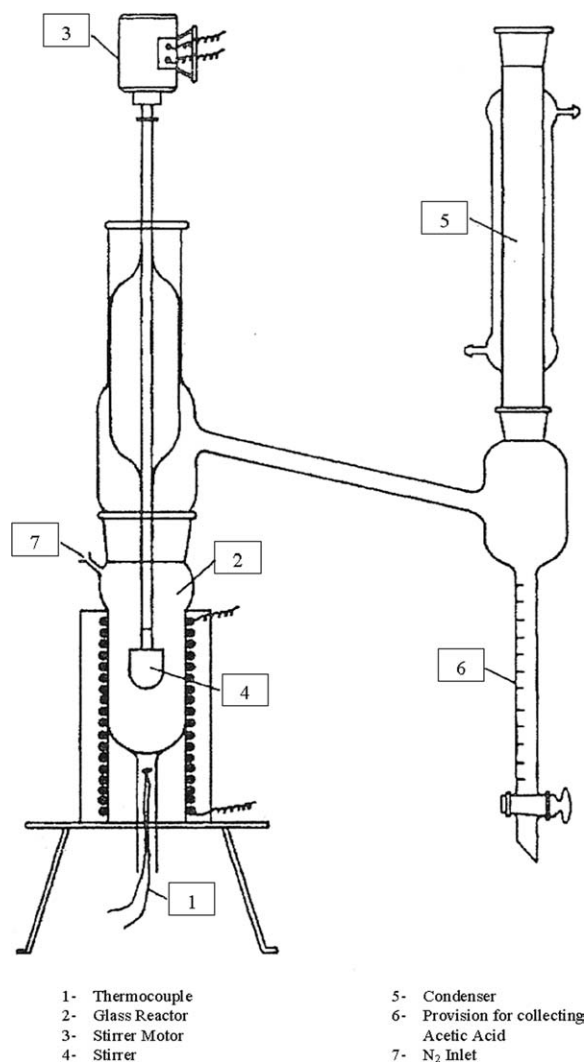
1- Thermocouple   5- Condenser
2- Glass Reactor   6- Provision for collecting
3- Stirrer Motor   Acetic Acid
4- Stirrer   7- N₂ Inlet

Figure 1 Glass-lined reactor used for the synthesis of the liquid crystalline polymers (recreated from Al-Haddad et al.[26]).

Three compounds reportedly used as catalysts (antimony trioxide, zinc acetate, and sodium acetate) are utilized to determine whether they cause the rate of reaction to be enhanced. Several models are used to characterize the polymerization kinetics.

EXPERIMENTAL

Materials

4-Acetoxy benzoic acid, sodium acetate, zinc acetate, and antimony trioxide (all of purity 99.5%) were obtained from Aldrich Chemicals, UK, and used as received. Polyethylene terephthalate (weight-average molecular weight of 38,000 and intrinsic viscosity of 0.6) was purchased from M/S Century Enka Pvt. Ltd. Pune, India.

Reactor assembly

A 250 mL glass-lined, electrically heated reactor was used for polymer synthesis. This reactor was assembled in the same manner reported by Al-Haddad et al.[26] The reactor had two ports, one for charging/stirring the reactants and the other for nitrogen purging. The temperature was maintained isothermally at the selected value. A provision was made for measuring the amount of the side product (acetic acid), as shown in Figure 1. The oligomers were then subjected to solid state polymerization by heating under vacuum in a 250-mL stainless steel parr reactor.

Polymer synthesis

Liquid crystalline polymer of three compositions (PET70/OB30, PET60/OB40, and PET50/OB50, weight/weight %) were synthesized. A dry nitrogen purge gas was used throughout the runs to prevent oxidation reactions. The temperatures chosen for the reactions were 260, 265, 270, and 275°C. Three compounds with reported catalytic effects (sodium acetate, zinc acetate and antimony trioxide) were used to determine whether they drive transesterification further to completion. Each catalyst was used at a concentration of 1 mol % of the total reaction batch. At this stage, all experiments were conducted at atmospheric pressure. The amount of 4-acetoxybenzoic acid lost by sublimation at 270 and 275°C was ignored, since it accounted for a maximum of 0.05% of the monomer charged.

The progress of the reaction was monitored by measuring the formation of the side product as a function of time. This was done by recording the readings on the calibrated provision attached to the reactor every 10 min. The reaction was assumed to be completed when the readings remained constant for 50 min. Gas chromatographic analyses were performed with a Perkin–Elmer model F-7 gas chromatograph equipped with flame ionization detector. A steel column (1 m long and 3 mm ID), packed with Porapak Q 120–150 mesh, was held at a temperature of 200°C. Nitrogen, flowing at 20 mL/min, was used as a carrier gas. The injection volume was 0.99 μL and pure acetic acid was used as an internal standard. At 260°C, the purity of acetic acid was almost 99%, whereas at 265, 270, and 275°C, it decreased to about 94%. The oligomers were washed with acetone to remove the unreacted 4-acetoxy benzoic acid. Solid state polymerization of the oligomers was carried out by heating the product in the parr reactor under vacuum (pressure less than 0.1 mmHg) for 8 h. No nitrogen flow was utilized during this process. The average degree of polymerization ($\overline{x_n}$) was estimated by correlating it to the moles of the side product generated. When $\overline{x_n}$ reached 4, the resulting

Figure 2 Nematic texture of PET50/OB50 observed under crossed polars at 210°C.
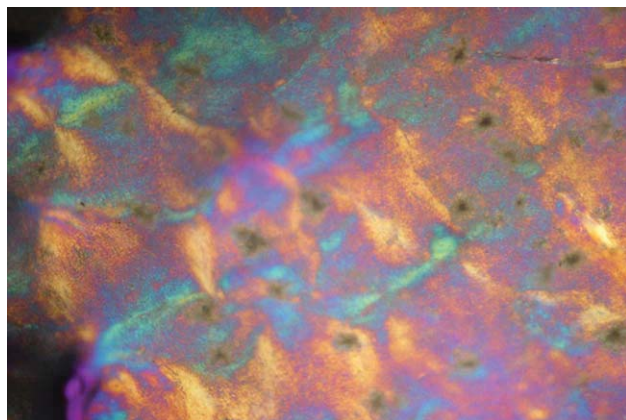

Figure 3 Nematic texture of PET70/OB30 observed under crossed polars at 210°C.

oligomers were meltable even at the highest temperature used in this experiment (275°C). However, solid state polymerization of the oligomers was not appreciable, as reflected in the minimal evolution of acetic acid at this stage.

Polymer characterization

Polarizing optical microscopy

All samples were examined with a Zeiss polarizing microscope, equipped with hot stage lenses. A Linkam hot-stage and allied temperature controller were used to heat and cool the sample at a controlled rate. The hot stage was heated at 10°C/min, with a cover slip resting on the heating block. A small fragment of the LCP sample was dropped on the hot glass, where it melted rapidly. A second cover slip was placed on top and the sample was flattened by tapping gently. This was necessary to lower the melt viscosity and obtain recognizable textures.

Thermogravimetric analysis

A thermogravimetric analysis of the synthesized LCP systems was carried out to assess their thermal durability using TA-SDT 2960 Thermobalance supplied by TA Instruments, U.K. A sample, placed in platinum cup, was subjected to heating at a rate of 10°C/min under a constant nitrogen flow of 25 mL/min while residual weight was simultaneously recorded as a function of temperature.

RESULTS AND DISCUSSION

Optical polarizing microscopy

The formation of liquid crystalline structure in the systems synthesized was confirmed using hot stage
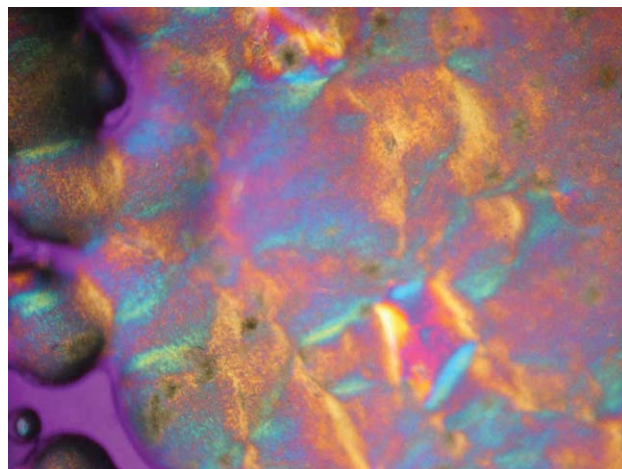
polarizing microscope. Figures 2 and 3 show the nematic textures obtained for uncatalyzed PET50/OB50 and PET70/OB30. Upon heating, viscous birefringent fluid was formed around 210°C, indicating the formation of a mesophase. These polymers exhibited streak textures that are consistent with the anisotropic mesomorphic phase observed in similar systems studied by Messiri et al.[27] PET70/OB30 and PET50/OB50 show typical threaded texture, a characteristic of the nematic phase of PET-oxybenzoate systems.[28] Figure 3 confirms the liquid crystal nature of the system containing the least amount of OB, i.e., 30 wt %. Most studies emphasize that the minimum amount needed to attain this phase is 35%, as suggested by Hibbs et al.[29]

Thermogravimetric analysis

It was noted that the liquid crystalline polymers degrade at lower temperatures compared to PET, as
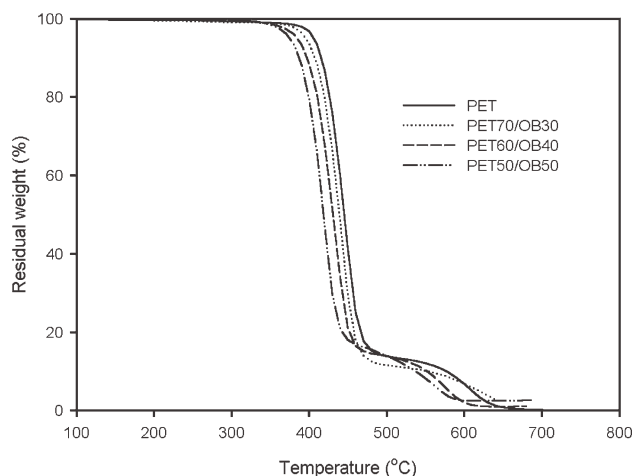

Figure 4 TG analysis of PET and PET/OB systems carried out at 10°C/min under nitrogen.
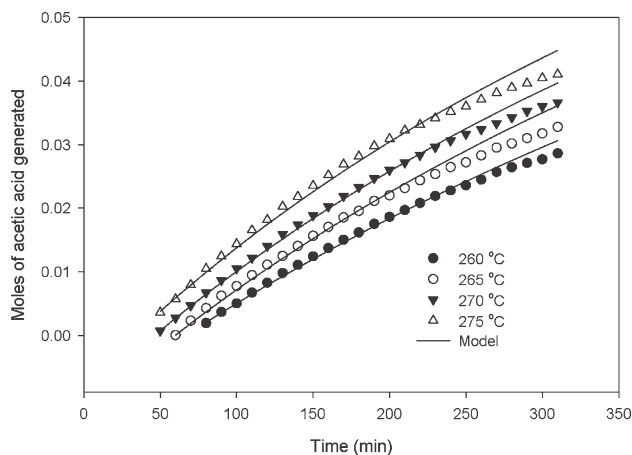
Figure 5 Nonlinear model application to the uncatalyzed polymerization of PET60/OB40.

Figure 6 Nonlinear model application to the polymerization of PET60/OB40 catalyzed with sodium acetate.

seen in Figure 4. The increase in PET content enhances the thermal stability of the polymers developed. Two-step degradation is noticed for both PET and the LCPs. A similar observation was made by Khan et al.,[30] who studied the thermal properties of LCPs synthesized from terephthalic acid, phenylhydroquinone, and napthalene diol. Some researchers sug-
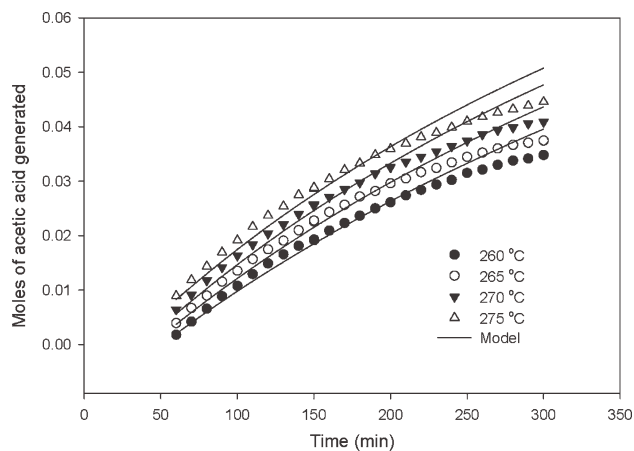
gested that degradation of LCPs proceeds through chain scission, hydrogen abstraction reactions, and the scission of the ester groups.[31] Others proposed different degradation mechanisms such as Fries-analogue rearrangements.[32] Degradation of the synthesized PET/OB systems starts around 380°C, which is lower than what has been reported in other LCPs.

TABLE I
Polymerization Kinetic Parameters Obtained Using the Nonlinear Model

System	Temp.(°C)	Uncatalyzed k (L mol^{-1} min^{-1})	t_o (min)	LnA	E (kJ mol^{-1})	ASE	Zinc acetate k (L mol^{-1} min^{-1})	t_o (min)	LnA	E (kJ mol^{-1})	ASE
PET70/OB30	260	3.26E-03	77.3			0.2179	1.07E-02	77.1			0.0834
	265	3.66E-03	68.3	5.5	49.8	0.2700	1.24E-02	69.8	8.0	55.3	0.2787
	270	4.08E-03	61.1			0.2362	1.43E-02	58.8			0.3132
	275	4.43E-03	53.7			0.4582	1.55E-02	43.9			0.1141
PET70/OB40	260	6.07E-03	66.8	5.3	57.0	0.0348	7.77E-03	55.6	7.5	54.7	0.0688
	265	7.27E-03	59.9			0.1438	8.88E-03	49.4			0.0976
	270	7.81E-03	46.4			0.0385	9.82E-03	42.2			0.0820
	275	8.76E-03	32.9			0.0542	1.09E-02	35.6			0.1099
PET50/OB50	260	4.64E-03	60.1	3.6	39.9	0.0171	5.28E-03	45.6	3.8	40.1	0.0162
	265	5.06E-03	47.5			0.0388	5.87E-03	38.0			0.0261
	270	5.55E-03	35.9			0.0697	6.31E-03	29.0			0.0288
	275	5.91E-03	22.2			0.0749	6.78E-03	19.5			0.0783

| System	Temp.(°C)	Sodium acetate k (L mol^{-1} min^{-1})	t_o (min)	LnA	E (kJ mol^{-1})	ASE	Antimony trioxide k (L mol^{-1} min^{-1})	t_o (min)	LnA	E (kJ mol^{-1})	ASE
PET70/OB30	260	1.33E-02	68.8	7.1	50.8	0.1127	2.47E-02	54.8	1.2	21.7	0.3025
	265	1.48E-02	57.6			0.1534	2.67E-02	45.5			0.3737
	270	1.59E-02	46.2			0.1324	2.71E-02	35.3			0.2347
	275	1.84E-02	39.3			0.2180	2.85E-02	27.9			0.1740
PET60/OB40	260	8.21E-03	50.6	4.9	43.1	0.1436	1.34E-02	46.5	4.9	55.6	0.3471
	265	9.13E-03	43.9			0.1923	1.37E-02	33.2			0.1827
	270	1.01E-02	37.6			0.2226	1.50E-02	24.7			0.2295
	275	1.07E-02	28.4			0.1649	1.72E-02	21.2			0.3996
PET50/OB50	260	5.60E-03	25.9	4.8	44.3	0.0783	8.11E-03	26.8	1.3	27.3	0.2492
	265	6.01E-03	16.2			0.2116	8.83E-03	21.1			0.3061
	270	6.81E-03	11.4			0.2331	9.35E-03	12.9			0.2657
	275	7.28E-03	2.1			0.1392	9.59E-03	2.7			0.2410
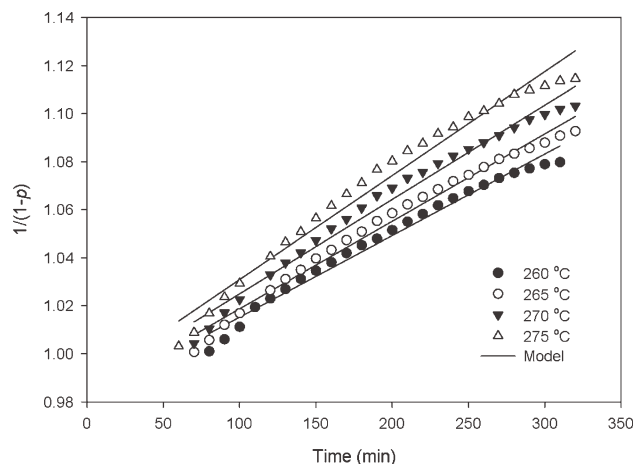
Figure 7 Second order model application to the uncatalyzed polymerization of PET70/OB30.

Polymerization kinetics

Nonlinear model

A nonlinear model was fitted to the polymerization data, in which the rate constant k was evaluated by minimizing the error between the measured and calculated moles of the side product. From the reaction stochiometery, it can be shown that the moles of the side product generated are equal to the moles of monomer reacted. Thus, the following equations can be utilized:

$$\sum \alpha = \frac{\upsilon_0}{1 + k\upsilon_0 t} \tag{3}$$

$$M_{ic} = \upsilon_0 - \sum \alpha \tag{4}$$

where $\sum\alpha$, υ_o, M_{ic} and k correspond to the amount of unreacted monomer (mole), the initial amount of monomer (mole), the amount of monomer reacted (mole) and rate constant, respectively.

Substituting for $\sum\alpha$ in eq. (4) gives:

$$M_{ic} = \frac{\upsilon_0^2 kt}{1 + \upsilon_0 kt} \tag{5}$$

In practical polymerization reactions, there is a delay (dead time) at the start of the experiment before any noticeable amount of side product is collected. This is generally attributed to the capacity of the reactor, rate of reaction, catalyst activity and temperature. To take this factor into account, eq. (5) is modified to yield:

$$M_{ic} = \frac{\upsilon_0^2 k(t - t_0)}{1 + \upsilon_0 k(t - t_0)} \tag{6}$$

where t_o is the dead time. As stated earlier, the stochiometery of this reaction equates the moles of monomer reacted (M_{ic}) to the amount of side product generated. Thus, modeling reaction kinetics can

be carried out based on the measurement of acetic acid evolved as a function of time. This approach was not found in our literature review.

Using "Solver," a built-in function in Microsoft Excel that is based on Newton-Raphson method,[33] eq. (6) was applied to determine the best values of k and t_o. The model's fitting to the polymerization data of the synthesized liquid crystalline polymers is shown in Figure 5. The model's predictions of the amount of acetic acid evolved do not accurately compare to the experimental data. This is especially true at high temperatures and at later reaction stages. Further deterioration in model accuracy is found for catalyzed reactions, as seen in Figure 6. The kinetic parameters presented in Table I also reflect this observation through the values of Average Squared Errors (ASE). As shown in Table I, these polymerization reactions experience long dead times. Higher temperatures are characterized with higher rate constants. The increase in temperature, however, is accompanied by a proportionate decrease in t_o. It is also observed that as PET content increases, t_o increases. The catalytic polymerization of PET70/OB30 is characterized with the highest k values.

Second order model

As mentioned earlier, second order rate equation has been proposed to model the acidic-catalyzed polyesterification. The integrated form of eq. (2) is given as:

$$\frac{1}{c} - \frac{1}{c_0} = kt \tag{7}$$

where c_0 and c correspond to the initial concentration of [COOH⁻], or the stochiometrically equivalent [OH⁻], and the concentration at time t, respectively. If p is the conversion at time t, c may be represented as:
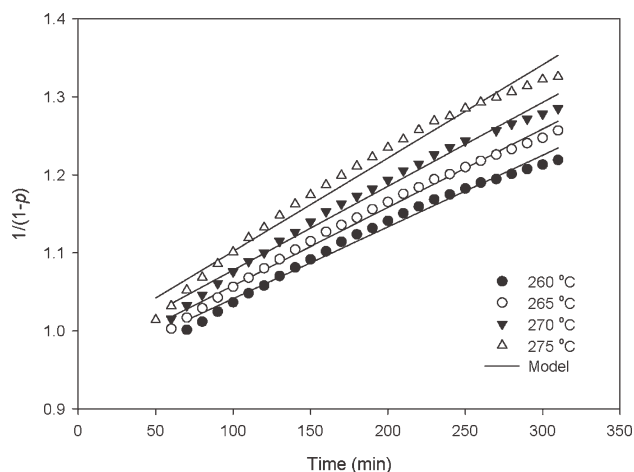

Figure 8 Second order model application to the polymerization of PET70/OB30 catalyzed with sodium acetate.

System	Temp. (°C)	Uncatalyzed				Zinc acetate			
		k (L mol^{-1} min^{-1})	E (kJ mol^{-1})	LnA	r^2	k (L mol^{-1} min^{-1})	E (kJ mol^{-1})	LnA	r^2
PET70/OB30	260	2.51E-03	101.1	16.5	0.9886	6.28E-03	99.7	17.4	0.9926
	265	3.35E-03			0.9855	1.01E-02			0.9926
	270	3.35E-03			0.9805	1.13E-02			0.987
	275	3.35E-03			0.9745	1.38E-02			0.9786
PET60/OB40	260	5.62E-03	71.6	10.7	0.9957	6.87E-03	52.7	5.1	0.9862
	265	6.24E-03			0.9953	7.49E-03			0.9875
	270	6.87E-03			0.9946	8.74E-03			0.9868
	275	8.11E-03			0.9901	9.36E-03			0.9888
PET50/OB50	260	4.47E-03	57.7	7.4	0.9976	4.96E-03	68.9	10.0	0.9957
	265	4.96E-03			0.9983	5.46E-03			0.9936
	270	4.96E-03			0.9975	5.95E-03			0.9941
	275	5.46E-03			0.9979	0.0065			0.991

System	Temp. (°C)	Sodium acetate				Antimony trioxide			
		k (L mol^{-1} min^{-1})	E (kJ mol^{-1})	LnA	r^2	k (L mol^{-1} min^{-1})	E (kJ mol^{-1})	LnA	r^2
PET70/OB30	260	1.13E-02			0.9782	1.88E-02			0.9724
	265	1.26E-02	71.6	11.4	0.9909	2.01E-02	58.4	9.1	0.972
	270	1.38E-02			0.9865	2.14E-02			0.9777
	275	1.51E-02			0.9795	2.39E-02			0.9739
PET60/OB40	260	6.87E-03	68.7	10.3	0.9864	9.99E-03	61.2	9.1	0.9758
	265	7.49E-03			0.9801	1.12E-02			0.9715
	270	8.11E-03			0.9817	1.19E-02			0.9627
	275	8.74E-03			0.9795	1.25E-02			0.9542
PET50/OB50	260	4.47E-03	73.2	11.1	0.9721	6.45E-03	53.9	7.1	0.9631
	265	4.96E-03			0.9736	6.95E-03			0.9569
	270	5.46E-03			0.975	7.44E-03			0.9543
	275	5.95E-03			0.976	7.44E-03			0.9486

$$c = c_0(1 - p) \qquad (8)$$

Upon substitution, eq. (8) becomes:

$$c_0 kt = \frac{1}{1 - p} - 1 \qquad (9)$$

where k can be calculated from the slope of the plot of $1/(1 - p)$ versus time. Sample plots are shown in Figures 7 and 8. This model generally does not follow the data points at the later reaction stages. The r^2 values presented in Table II lead to the same conclusion. Generally, the increase in reaction
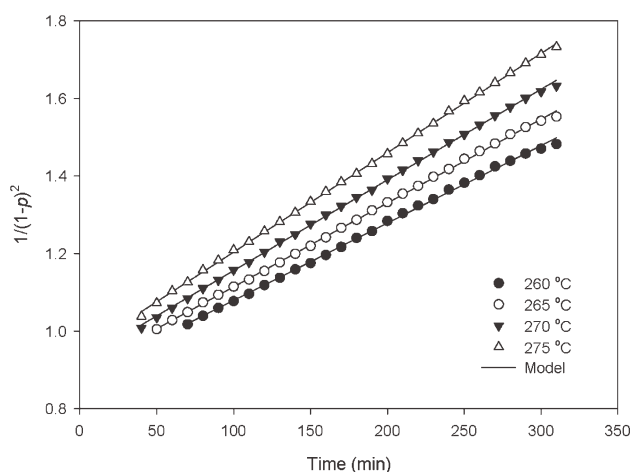

Figure 9 Third order model application to the uncatalyzed polymerization of PET50/OB50.
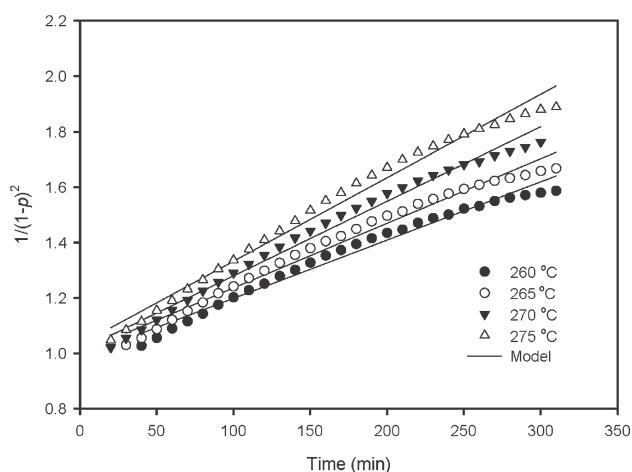

Figure 10 Third order model application to the polymerization of PET50/OB50 catalyzed with sodium acetate.

TABLE III
Polymerization Kinetic Parameters Obtained Using the Third Order Model

System	Temp. °C	Uncatalyzed k (L^2 mol^{-2} min^{-1})	E (kJ mol^{-1})	LnA	r^2	Zinc acetate k (L^2 mol^{-2} min^{-1})	E (kJ mol^{-1})	LnA	r^2
PET70/OB30	260	2.46E-02			0.9905	1.34E-01			0.9956
	265	2.81E-02	39.4	5.2	0.9882	1.42E-01	63.6	12.3	0.9963
	270	2.81E-02			0.9838	1.66E-01			0.9922
	275	3.16E-02			0.9781	1.97E-01			0.9855
PET60/OB40	260	1.03E-04	65.1	11.5	0.9982	5.06E-02	57.7	10.0	0.992
	265	4.48E-02			0.9981	5.65E-02			0.9933
	270	5.06E-02			0.9981	6.43E-02			0.9935
	275	5.84E-02			0.9956	7.21E-02			0.9959
PET50/OB50	260	2.46E-02	40.4	5.4	0.9989	2.83E-02	47.1	7.1	0.9978
	265	2.71E-02			0.9995	3.20E-02			0.9961
	270	2.83E-02			0.9995	3.45E-02			0.9974
	275	3.20E-02			0.9996	3.82E-02			0.9956

System	Temp. °C	Sodium actate k (L^2 mol^{-2} min^{-1})	E (kJ mol^{-1})	LnA	r^2	Antimony trioxide k (L^2 mol^{-2} min^{-1})	E (kJ mol^{-1})	LnA	r^2
PET70/OB30	260	1.66E-01	46.0	8.5686	0.9921	2.92E-01	45.6	9.0	0.9834
	265	1.81E-01			0.9956	3.08E-01			0.9845
	270	1.97E-01			0.9925	3.39E-01			0.9891
	275	2.21E-01			0.9879	3.87E-01			0.9862
PET60/OB40	260	5.06E-02	44.0	6.9445	0.9925	7.79E-02	43.5	7.3	0.9872
	265	5.45E-02			0.9881	8.57E-02			0.9834
	270	6.04E-02			0.9904	9.55E-02			0.9801
	275	6.62E-02			0.9892	1.01E-01			0.972
PET50/OB50	260	2.59E-02	57.9	9.39	0.9802	3.82E-02	33.9	4.4	0.9748
	265	2.83E-02			0.9822	4.06E-02			0.97
	270	3.20E-02			0.9832	4.43E-02			0.9677
	275	3.69E-02			0.9852	4.68E-02			0.9625

temperature is associated with an increase in the values of k. This is in agreement with the findings of Vulic and Schulpen,[34] Mathew et al.[35] and Williams et al..[3] However, this is not observed for the uncatalyzed polymerization of PET70/OB30. Once again,

Figure 11 Second order model (with breaks) application to the polymerization of PET70/OB30 catalyzed with sodium acetate.

catalyzed PET70/OB30 systems exhibit the highest rate constant values.

Third order model

Adopting third-order kinetics for polyesterification, the integration of eq. (1) between the limits c_0 and c gives:

$$2kt = \frac{1}{c^2} - \frac{1}{c_0^2} \qquad (10)$$

When substituting eq. (8) into eq. (10), the following expression results:

$$2c_0^2 kt = \frac{1}{(1-p)^2} - 1 \qquad (11)$$

where k can be calculated from the slope of $1/(1-p)^2$ versus time. Equation (11) is obtained by Flory[1] for third order polyesterification reactions. As seen in Figures 9 and 10, third-order kinetics describe the reaction of PET/OB systems better than the previously examined models. Table III presents the kinetic parameters obtained from this analysis. The
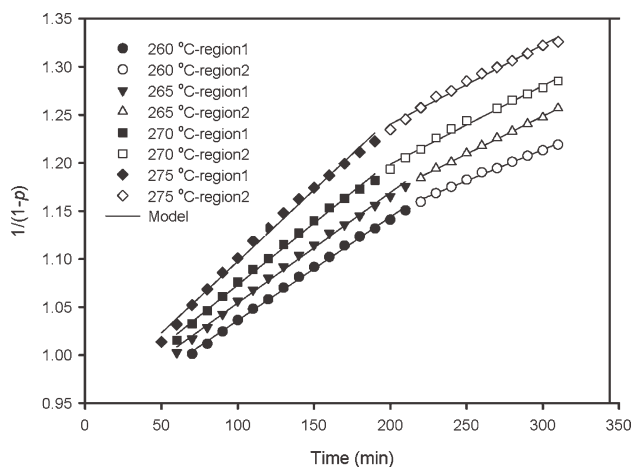
Polymerization Kinetic Parameters Obtained Using the Second Order Model with Breaks

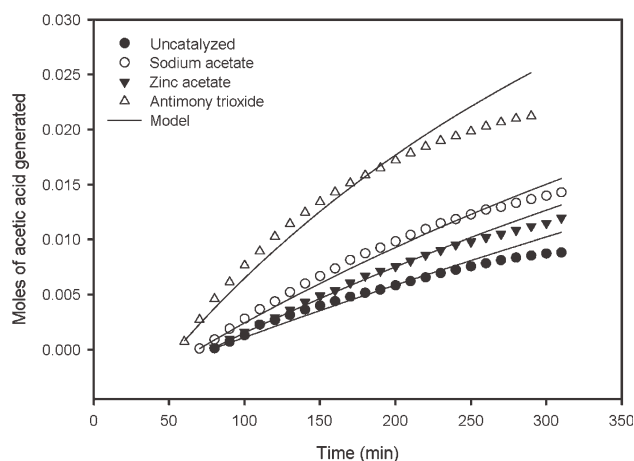| System	Catalyst	Temp. (°C)	Region 1				Region 2			
			k (L mol^{-1} min^{-1})	r^2	E (kJ mol^{-1})	LnA	k (L mol^{-1} min^{-1})	r^2	E (kJ mol^{-1})	LnA
PET70/OB30	Antimony trioxide	260	2.00E-03	0.99	32.6	5.0	1.00E-03	0.99	42.5	6.2
		265	2.10E-03	0.99			1.10E-03	0.99		
		270	2.10E-03	0.99			1.20E-03	0.99		
		275	2.40E-03	0.99			1.30E-03	0.99		
	Zinc acetate	260	9.00E-04	0.99	90.2	13.2	6.00E-04	0.99	52.1	7.4
		265	9.00E-04	0.99			7.00E-04	0.99		
		270	1.10E-03	0.99			7.00E-04	0.98		
		275	1.30E-03	0.99			6.00E-04	0.98		
	Sodium acetate	260	1.10E-03	0.99	76.1	10.2	6.00E-04	0.99	69.5	8.3
		265	1.10E-03	0.99			8.00E-04	0.99		
		270	1.30E-03	0.99			8.00E-04	0.99		
		275	1.50E-03	0.99			8.00E-04	0.99		
PET60/OB40	Uncatalyzed	260	9.00E-04	0.99	58.2	6.1				
		265	1.00E-03	0.99						
		270	1.10E-03	0.99						
		275	1.30E-03	0.99						
	Antimony trioxide	260	2.10E-03	0.99	35.3	1.8	1.20E-03	0.99	48.3	3.9
		265	2.20E-03	0.99			1.10E-03	0.99		
		270	2.40E-03	0.99			1.00E-03	0.99		
		275	2.60E-03	0.98			1.10E-03	0.98		
	Zinc acetate	260	1.30E-03	0.99	45.6	3.6	8.00E-04	0.99	51.6	4.5
		265	1.40E-03	0.99			9.00E-04	0.99		
		270	1.60E-03	0.99			1.00E-03	0.99		
		275	1.70E-03	0.99			1.10E-03	0.99		
	Sodium acetate	260	1.30E-03	0.99	50.6	4.8	8.00E-04	0.99	54.7	5.1
		265	1.50E-03	0.99			8.00E-04	0.98		
		270	1.60E-03	0.99			9.00E-04	0.99		
		275	1.80E-03	0.99			1.00E-03	0.99		
PET50/OB50	Antimony Trioxide	260	1.70E-03	0.98	26.3	1.4	8.00E-04	0.98	41.9	2.1
		265	1.80E-03	0.99			7.00E-04	0.99		
		270	1.90E-03	0.98			7.00E-04	0.96		
		275	2.00E-03	0.98			6.00E-04	0.97		
	Zinc acetate	260	1.10E-03	0.99	39.1	2.0	9.00E-04	0.99	51.2	4.4
		265	1.20E-03	0.99			9.00E-04	0.98		
		270	1.30E-03	0.99			1.00E-03	0.99		
		275	1.40E-03	0.99			9.00E-04	0.98		
	Sodium acetate	260	1.20E-03	0.99	36.3	1.5	6.00E-04	0.97	36.3	1.5
		265	1.20E-03	0.99			6.00E-04	0.98		
		270	1.40E-03	0.99			7.00E-04	0.99		
		275	1.50E-03	0.99			7.00E-04	0.98		

Figure 12 Nonlinear model application to the catalyzed polymerization of PET70/OB30 at 260°C.
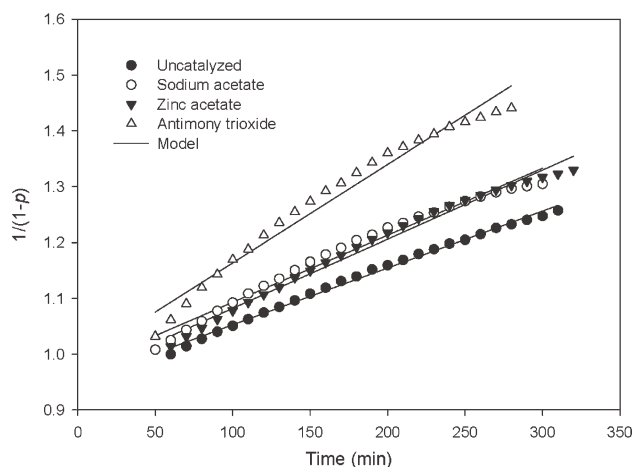

Figure 13 Second order model application to the polymerization of PET60/OB40 at 265°C.
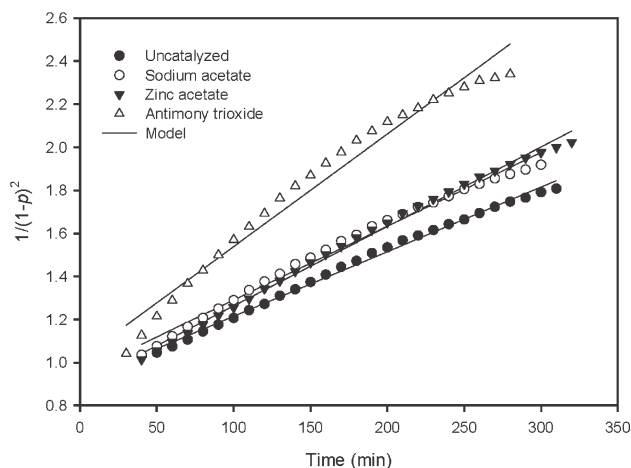
Figure 14 Third order model application to the polymerization of PET60/OB40 at 275°C.

slightly proportional relationship between reaction temperature and rate constant is reflected in this model as well. PET70/OB30 systems resulting from catalyzed reactions have the highest rate constant values relative to reaction temperature.

Second order with breaks

Based on a method proposed by Lodha et al.,[6] the kinetic data was divided into two regions and fitted separately to the second order rate equation. Figure 11 is a representative plot of this method and the fitting results are shown in Table IV. Second-order kinetics can now adequately represent the data. r^2 values obtained for both regions are generally higher than those of the other models investigated. The data of uncatalyzed reactions can be treated essentially as one region. The break in the data range for catalyzed reactions is attributed to the change in reaction mechanism. Breaks appearing in the plots of $1/(1 - p)$ versus time have been reported in many copoly-
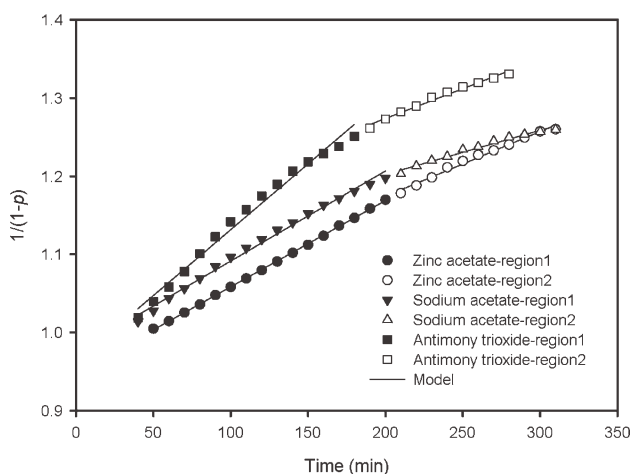

Figure 15 Second order model (with breaks) application to the catalyzed polymerization of PET50/OB50 at 260°C.
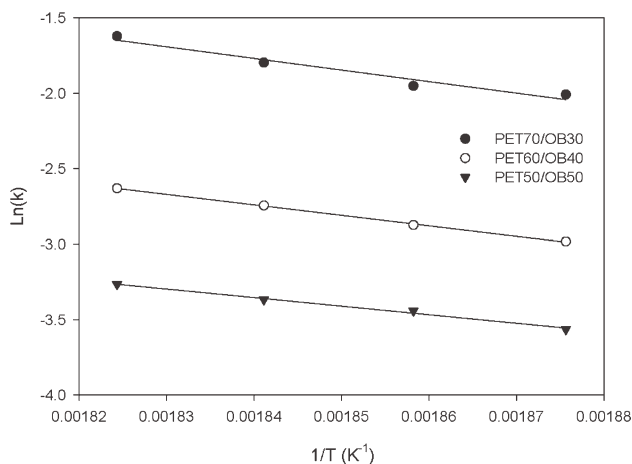
Figure 16 Determination of activation energy for the polymerization of PET/OB systems catalyzed with zinc acetate using third order rate constants.

merization systems.[3] Rate constant values, though, are generally lower in comparison and tend to increase in the second region. This observation agrees well with the work reported by Mathew et al.[35] but contradicts with the conclusions of Williams et al..[3] This validates the assumption that heterogeneous systems tend to have slower reaction. Higher temperatures are associated with a slight increase in k values for both regions. In general, PET60/OB40 displays the highest k values.

Influence of catalysts

The kinetic data of the systems catalyzed by antimony trioxide is difficult to model, as shown in the *ASE* and r^2 values indicated in Tables I to III. Reactions catalyzed with zinc acetate, on the other hand, are readily and more accurately modeled. Figures 12 to 14, which are representative plots of the fitting of the nonlinear, second-order and third-order models to the catalyzed reactions, also support these observations. But when the kinetic data sets are divided into two regions, as shown in Figure 15, the accelerating effect of antimony trioxide on reaction rate becomes more obvious and dominant compared to zinc acetate and sodium acetate. Overall, the presence of the catalyst enhanced the rate of polyesterification by altering the reaction mechanism.

Determination of activation energy

Activation energy is most commonly represented by the Arrhenius equation:

$$\mathrm{Ln}(k) = \mathrm{Ln}(A) - \frac{E}{RT} \qquad (12)$$

where A is the pre-exponential factor, T is the temperature (K), R is the ideal gas constant (J mol^{-1} K)

and E is the activation energy (J mol^{-1}). By plotting Ln(k) versus $1/T$, E is calculated from the slope while Ln(A) is obtained from the intercept. A representative plot of the Arrhenius equation is given in Figure 16. The E values determined using the nonlinear model do not exhibit any characteristic trend with either the LCP composition or the type of catalyst, as shown in Table I. Ln(A), however, generally increases as PET content increases. The systems presented in Table III show two behaviors: uncatalyzed reactions and reactions catalyzed with sodium acetate have a random pattern of E values, while reactions catalyzed with antimony trioxide and zinc acetate have an upward trend between E and PET content. The same observations apply to Ln(A) values. Chung et al.[36] reported an opposite trend, where the activation energy of copolymerization was lowered with the addition of catalysts. The higher activation energies of catalyzed reactions may be explained in light of absolute rate theory. The entropy factors outweigh the increase in reaction enthalpy, as evidenced in the increase in rate constant values, which results in driving the reaction forward.

CONCLUSIONS

Liquid crystalline polymers were developed using polyethylene terephthalate and 4-acetoxy benzoic acid. Three compositions were synthesized: PET70/OB30, PET60/OB40 and PET50/OB50 (wt/wt %). The presence of LCP structures in the developed systems was confirmed through optical polarizing microscopy. TGA analysis indicates that the liquid crystalline polymers degrade at lower temperatures compared to the neat PET.

The polymerization kinetics of the synthesized PET/oxybenzoate liquid crystalline polymers was studied. The kinetic data of acetic acid evolved during reaction as a function of time exhibit a sigmoidal shape. Four approaches were investigated to model the reaction kinetics: a nonlinear model, second-order model, third-order model, and second-order model with breaks. The latter method was found to describe the kinetic data more accurately. The rate of reaction, represented by the rate constant, was found to be proportionally related to reaction temperature. The catalyzing effect of antimony trioxide, zinc acetate and sodium acetate was examined. Our data shows that antimony trioxide induced a more pronounced impact on the kinetic rate of these reactions.

References

1. Jackson, W. Mol Cryst Liq Cryst 1989, 169, 23.
2. Hamb, F. L. J Polym Sci Part A-1: Polym Chem 1972, 10, 3217.
3. Williams, P. A.; Han, X.; Padias, A. B.; Hall, H. K. Macromolecules 1996, 29, 1874.
4. Han, X.; Williams, P. A.; Padias, A. B.; Hall, H. K.; Linstid, H. C.; Sung, H. N.; Lee, C. Macromolecules 1996, 29, 8313.
5. Mathew, J.; Bahulekar, R. V.; Ghadage, R. S.; Rajan, C. R.; Ponrathnam, S.; Prasad, S. D. Macromolecules 1992, 25, 7338.
6. Lodha, A.; Ghadage, R. S.; Ponrathnam, S. Polymer 1997, 38, 6167.
7. Flory, P. J. J Am Chem Soc 1937, 59, 466.
8. Colonge, J.; Stuchlik, P. Bull Soc Chim 1950, 17, 267.
9. Davies, M. Research (London) 1949, 2, 544.
10. Tang, A. C.; Yao, K. S. J Polym Sci 1959, 35, 219.
11. Hartman, R. J.; Borders, A. M. J Am Chem Soc 1937, 59, 2107.
12. Goldschmidt, H.; Ulby, O. Z Phys Chem 1907, 60, 728.
13. Flory, P. J. Principles of Polymer Chemistry; Ithaca, New York: Cornell University Press, 1953.
14. Carothers, W. H.; Natta, F. J. J Am Chem Soc 1930, 52, 314.
15. Rolfe, R. T.; Hinshelwood, C. N. Trans Faraday Soc 1934, 30, 935.
16. Fradet, A.; Marechal, E. Adv Polym Sci 1982, 43, 51.
17. Fradet, A.; Marechal, E. J Polym Sci Polym Chem Ed 1981, 19, 2905.
18. Fradet, A.; Marechal, E. J. Macromol Sci Chem A 1982, 17, 859.
19. Pedretti, U.; Bresci, B.; Bonfanti, C.; Magagnini, P. L.; Roggero, A. U.S. Pat. 5,086,160 (1992).
20. East, A. J.; Charbonneau, L. F.; Calundann, G. W. U.S. Pat. 4,330,457 (1982).
21. Charbonneau, L. F. U.S. Pat. 4,429,105 (1984).
22. Pielartzik, H.; Brinkmeyer, H.; Meyer, R. V.; Willenberg, B. U.S. Pat. 5,084,547 (1992).
23. Charbonneau, L. F.; Calundann, G. W. U.S. Pat. 5,171,823 (1992).
24. Calundann, G. W. U.S. Pat. 4,161,470 (1979).
25. Jin, J. I.; Antoun, S.; Ober, C.; Lenz, R. W. Br Polym J 1980, 12, 132.
26. Al-Haddad, A.; Mathew, J.; Elkamel, A.; El-Nagdi, M. J Appl Polym Sci 1999, 72, 467.
27. Messiri, W.; Menczel, J.; Gaur, U.; Wunderlich, B. J Polym Sci Polym Phys Ed 1982, 20, 719.
28. Shinn, H. T.; Lin, C. C. J Appl Polym Sci 1993, 49, 1093.
29. Hibbs, M. R.; Vargas, M.; Holtzclow, J.; Rich, W.; Collard, D.; Schiraldi, D. A. Macromolecules 2003, 36, 7543.
30. Khan, A.-R.; Mathew, J.; AL-Shayji, K.; Sari, M. Eur Polym J 2002, 38, 1013.
31. Crossland, B.; Knight, G. J.; Wright, W. W. Br Polym J 1986, 27, 1992.
32. Hummel, D. O.; Neuhoff, U.; Bretz, A.; Dussel, H.-J. Makromol Chem 1993, 194, 1545.
33. Chapra, S. C.; Canale, R. P. Numerical Methods for Engineers, 3rd ed.; McGraw Hill: New York, 1998.
34. Vulic, I.; Schulpen, T. J Polym Sci Part A: Polym Chem 1992, 30, 2725.
35. Mathew, J.; Ghadge, R. S.; Ponrathnam, S.; Prasad, S. D. Macromolecules 1994, 27, 4021.
36. Chung, T.-S.; Cheng, S.-X. J Polym Sci 2000, 38, 1257.